

Specific sequences from the carboxyl terminus of human p53 gene product form anti-parallel tetramers in solution

(oligomerization/coiled-coil/four-helical bundle/tumor-suppressor gene)

HIROSHI SAKAMOTO[†], MARC S. LEWIS[‡], HIROAKI KODAMA[§], ETTORE APPELLA^{†¶},
AND KAZUYASU SAKAGUCHI^{†¶}

[†]Laboratory of Cell Biology, National Cancer Institute, and [‡]Biomedical Engineering and Instrumentation Program, National Center for Research Resources, Bethesda, MD 20892; and [§]Laboratory of Biochemistry, Faculty of Science and Engineering, Saga University, Saga 840, Japan

Communicated by Gary Felsenfeld, May 16, 1994 (received for review March 16, 1994)

ABSTRACT Human p53 is a tumor-suppressor gene product associated with control of the cell cycle and with growth suppression, and it is known to form homotetramers in solution. To investigate the relationship of structure to tetramerization, nine peptides corresponding to carboxyl-terminal sequences in human p53 were chemically synthesized, and their equilibrium associative properties were determined by analytical ultracentrifugation. Secondary structure, as determined by circular dichroism measurements, was correlated with oligomerization properties of each peptide. The sedimentation profiles of peptides 319–393 and 319–360 fit a two-state model of peptide monomers in equilibrium with peptide tetramers. Successive deletion of amino- and carboxyl-terminal residues from 319–360 reduced tetramer formation. Further, substitution of alanine for Leu-323, Tyr-327, and Leu-330 abolished tetramerization. Circular dichroism studies showed that peptide 319–351 had the highest α -helix content, while the other peptides that did not form tetramers had low helical structure. These studies define a minimal region and identify certain critical residues involved in tetramerization. Cross-linking studies between monomer units in the tetramer suggest that the helices adopt an anti-parallel arrangement. We propose that conformational shifts in the helical structure of the p53 tetramerization domain result in a repositioning of subunits relative to one another. This repositioning provides an explanation relating conformational changes at the carboxyl terminus with changes in sequence-specific DNA binding by the highly conserved central domain.

The p53 gene product is a phosphoprotein which has been implicated in the regulation of cell proliferation. Functional inactivation of the protein either by association with viral proteins (1) or, more frequently, by point mutations, as found in many human tumors, leads to cellular transformation (2). Wild-type p53 exhibits trans-activation of transcriptional activity which is thought to mediate its anti-proliferation activity (3). At the biological level, p53 undergoes oligomerization, and it can adopt two distinct conformational states, with low or high affinity for site-specific DNA binding (4). Many of the p53 mutants associated with human tumors appear to be incapable of binding DNA and can be distinguished from wild-type p53 by their oligomerization state and by their "mutant" immunoreactivity (5–7).

Recent structure–function analyses of p53 have mapped the trans-activation domain to the 42 amino (N)-terminal amino acids (8). This region is highly susceptible to proteolytic digestion and may be loosely folded in the absence of ligand (9). Deletion analysis has shown that residues 90–286 form a stable domain which binds DNA with specificity (4).

Subtilisin treatment of the p53 protein generates a 191-amino acid protease-resistant monomeric fragment from the mid-section that corresponds to a highly conserved region in which the majority of missense mutations occur (9, 10).

We have a limited understanding of the relationship between oligomerization and DNA-binding activity. The oligomerization domain of p53 has been mapped to the carboxyl (C) terminus; p53 lacking the 47 C-terminal amino acids is monomeric rather than tetrameric (11). Further studies have implicated the presence of two distinct regions in the C terminus as sufficient for tetramer formation (12). In the present study, we have synthesized nine different peptides within the domain encompassed by residues 303–393 of the native protein and studied their equilibrium oligomerization states *in vitro*. A core peptide of 42 amino acids (residues 319–360) exhibits the strongest tetramerization. It also exhibits significant structure and forms a unique antiparallel four-helical bundle. A 24-residue basic region (residues 363–386) is not necessary for tetramer formation. Further, the core peptide contains critical residues in the N terminus necessary for tetramerization and α -helix formation. These results suggest that the functional domain controlling oligomerization in p53 is limited to a relatively small sequence of amino acids near the C terminus. On the basis of the observed association, a model is proposed relating tetramer formation to DNA binding.

MATERIALS AND METHODS

Chemical Synthesis of p53 Peptides. The p53 peptides [sequences 319–347, 319–351, 319–360, 332–360, 360–393, Ac-Cys-Gly-Gly-319–351 (AC), and Bz-319–351-Gly-Gly-Cys (BC)] were synthesized by the solid-phase method, using fluoren-9-ylmethoxycarbonyl (Fmoc) chemistry on an Applied Biosystems 430A peptide synthesizer. Cleavage of the peptides from the resin and removal of the side-chain protecting groups were accomplished by using reagent K (13).

The larger peptides [sequences 303–393, 319–393, [Ala^{323, 327, 330}]319–393 (319AAA–393), and 335–393] were synthesized by a segment condensation method using appropriate peptide thioesters (14, 15). Peptide thioesters, corresponding to residues 303–334, 319–334, 319AAA–334, and 335–360, were synthesized with *t*-Boc chemistry, using *t*-Boc-Gly-SCH₂CH₂CO-Ala-4-methylbenzhydramine (MBHA) resin and cleaved by HF/*p*-cresol. After all the lysine side chains of the peptides were protected by *t*-Boc

Abbreviations: AC, N-terminal-extended p53 peptide Ac-Cys-Gly-Gly-319–351; BC, C-terminal-extended p53 peptide Bz-319–351-Gly-Gly-Cys; 319AAA–393, Ala-substituted p53 peptide [Ala^{323, 327, 330}]319–393.

[¶]To whom reprint requests should be addressed at: Laboratory of Cell Biology, National Cancer Institute, Building 37, Room 1B10, Bethesda, MD 20892.

The publication costs of this article were defrayed in part by page charge payment. This article must therefore be hereby marked "advertisement" in accordance with 18 U.S.C. §1734 solely to indicate this fact.

groups, the peptide thioesters were successively condensed with the C-terminal portion (sequence 361–393) in dimethyl sulfoxide in the presence of AgNO₃ and *N*-hydroxysuccinimide. Deprotection of the final peptides was accomplished by using trifluoroacetic acid/ethanedithiol.

All the synthetic peptides were purified by HPLC on a Vydac C-4 column with 0.05% trifluoroacetic acid/water/acetonitrile, and their composition and mass were confirmed by amino acid analysis and mass spectroscopy.

Analytical Ultracentrifugation. Analytical ultracentrifugation was carried out in a Beckman XL-A analytical ultracentrifuge. The buffer was 50 mM Tris·HCl, pH 7.5/100 mM NaCl. Rotor speeds ranged from 24,000 to 32,000 rpm, depending on the molar mass of the peptide studied. The equilibrium distributions of the oligomeric species were measured over a range of temperatures from 5°C to 33°C. With column lengths of approximately 5 mm, 40 hr was allowed for the initial equilibrium and 12 hr was allowed for reequilibration after temperature changes. All scans were performed at 231 nm. The extinction coefficients of the peptides at 231 nm were calculated from the absorbances at 231 nm and the concentrations of the peptide solutions. The data were edited by using the XL-A software and analyzed by mathematical modeling using MLAB (Civilized Software, Bethesda, MD) to perform nonlinear least-squares curve fitting of the data with appropriate models.

The general mathematical model for fitting the data has the form

$$A_r = A_{b,1} \exp[AM_1(r^2 - r_b^2)] + A_{b,1}^2 \exp[\ln k_{12} + 2AM_1(r^2 - r_b^2)] + A_{b,1}^4 \exp[\ln k_{14} + 4AM_1(r^2 - r_b^2)] + \epsilon.$$

The use of $\ln k$ precludes obtaining negative values for k_{12} and k_{14} ; the curve fitting returns a large negative number for an absent species. A_r refers to the total absorbance as a function of radial position. $A_{b,1}$ is the absorbance of monomer at r_b , the radial position from the cell bottom. $A = (1 - \phi^* \rho) \omega^2 / 2RT$, where ϕ^* is the compositional partial specific volume of the peptide, ρ is the solvent density, ω is the angular velocity of the rotor, R is the gas constant, and T is the absolute temperature. M_1 is the molecular mass of the monomer and ϵ is a small baseline error correction term.

This model is written in terms of an equilibrium constant on an absorbance concentration scale, where $k_{12} = A_2/A_1^2$ and $k_{14} = A_4/A_1^4$; for thermodynamic calculations these must be converted to a molar scale by using $\ln K_{12} = \ln k_{12} + \ln(E_1/2)$ and $\ln K_{14} = \ln k_{14} + \ln(E_1^3/4)$, where E_1 is the molar extinction coefficient of the peptide monomer at 231 nm. This relationship assumes that the molar extinction coefficient for the peptide dimer, $E_2 = 2E_1$ and for the tetramer $E_4 = 4E_1$. This model also assumes that the apparent partial specific volumes of the monomer and the oligomers are identical.

The values of M_1 , the molecular mass of the peptide monomer, and the values of ϕ^* , the apparent compositional partial specific volume of the peptide, were calculated from the amino acid sequence of the peptides for a temperature of 25°C, using the values of Zamyatin (16). The values of ϕ^* at other temperatures were calculated by using a value of $0.00035 \text{ cm}^3 \cdot \text{g}^{-1} \cdot \text{deg}^{-1}$ for $\Delta\phi^*/\Delta T$. The values of the density of the buffer at the different temperatures were calculated from standard density tables.

Circular Dichroism. The CD spectra were recorded on a JASCO J-720 spectropolarimeter with a 1-mm pathlength cuvette. The instrument was calibrated with recrystallized *d*-10-camphorsulfonic acid. All spectra were recorded from 20 μM solutions of the peptides in 50 mM sodium phosphate buffer, pH 7.5 at 20°C. The CD spectra are presented as a plot of the residue ellipticity as a function of wavelength.

Determination of Tetramer Orientation. All solutions used in this experiment were degassed and flushed with helium to avoid oxidation of cysteine residues. Solutions of AC and of BC were prepared in 0.05% trifluoroacetic acid. The peptide solutions were mixed and diluted with water, 10 \times buffer was added, and the mixture was incubated for 30 min at room temperature. The final solution contained 20 mM Tris·HCl, pH 7.5, 100 mM NaCl, and each peptide at 50 μM . After the addition of 1,6-bismaleimidohexane (50 μM), the reaction mixture was incubated for 1 hr at room temperature and analyzed by HPLC on a Beckman Ultrasphere C₈ column.

RESULTS

Analytical Ultracentrifugation of Human p53 C-Terminal Fragments. The various C-terminal peptide domains of p53 could be clearly classified into two categories: those peptides that were only monomeric and those that were capable of reversible homogeneous association. Peptides 335–393, 332–360, and 319AAA–393 were found to be monomeric; the curve-fitting procedure rejected the possible presence of either dimer or tetramer. Of the remaining peptides, with the exception of 319–347, all were found to be in monomer–tetramer equilibria. In every case, the analysis returned very large negative numbers for $\ln k_{12}$, implying zero values for k_{12} ,

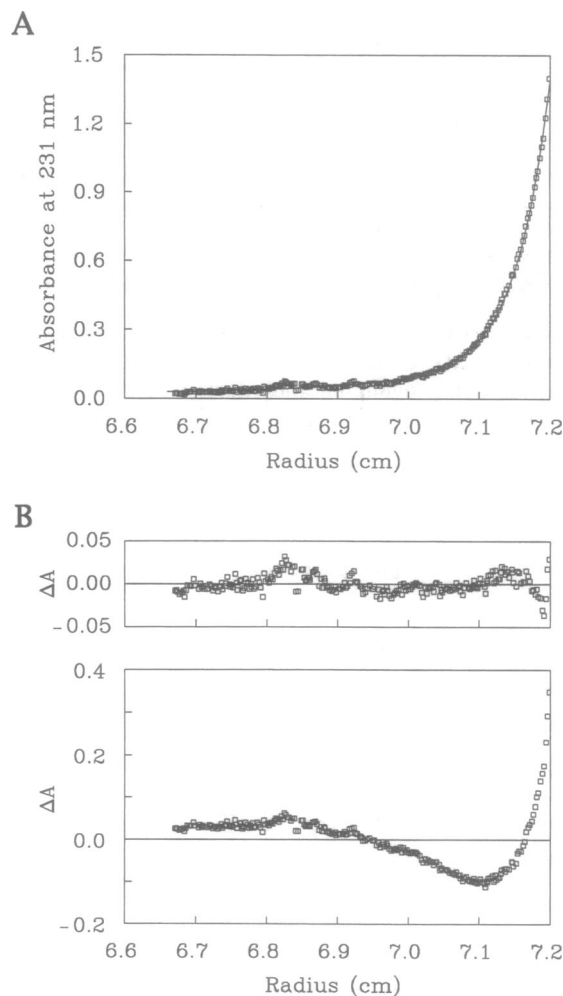


FIG. 1. Distributions of concentration and residuals of the p53 fragment 303–393 at centrifugal equilibrium at 24,000 rpm, 24°C, and pH 7.5. (A) Concentration distribution fit as a monomer–tetramer equilibrium model. (B) (Upper) Distribution of the residuals for the concentration fit as a monomer–tetramer. (Lower) Distribution of the residuals for the concentration fit as a monomer–dimer.

and precluding the possibility of monomer-dimer or monomer-dimer-tetramer as association models. Fig. 1 illustrates the fit of a monomer-tetramer model to the data for the largest peptide, 303-393. For purposes of illustration, the distribution of residuals for this model is shown with the distribution for a forced fit of this data with a monomer-dimer model ($\ln k_{14}$ set to a large negative number and not varied). The inferiority of this model is obvious. Peptide 319-347 could be fit as a monomer-dimer, monomer-dimer-tetramer, or monomer-tetramer. However, on the basis of the criteria of minimum sum of squares, minimum standard errors of the parameters, and most random distribution of residuals, the monomer-tetramer model was optimal. The other models could be fit only because the association was quite weak.

For those peptides which exhibited association, the values of ΔG° , ΔS° , ΔH° , ΔC_p° , and $d\Delta C_p^\circ/dT$ were obtained by the procedure of Clarke and Glew (17), which involves expressing ΔH° and ΔC_p° as Taylor series expansions around a reference temperature of 20°C. Only the values of ΔG° at 20°C are reported here; the other values will be reported in a subsequent publication.

Fig. 2 presents our results demonstrating the effects of truncation and amino acid substitutions on the tetramerization of synthetic p53 peptides. The sequence 303-393 is used as a reference structure for purpose of discussion. N-terminal truncation of the peptide enhanced association with an increase of ΔG° of 0.62 kcal·mol⁻¹ ($K_{D,303-393}/K_{D,319-393} = 1.42$), suggesting that residues between 303 and 319 have a modest inhibitory effect on tetramerization. Deletion of another 16 amino acids abolished tetramerization, demonstrating that at least some of the amino acids between residues 319 and 335 are essential for tetramer formation. This is supported by the fact that a variant of 319-393 in which Leu-323, Tyr-327, and Leu-330 were replaced by alanines (319AAA-393) also failed to form a tetramer.

Comparison of 319-393 with 319-360 shows that deletion of 33 C-terminal amino acids has no effect on the tetramerization, since the values of ΔG° are equivalent within experimental error. Comparison of 303-393 with 303-360 indicates a decrease in ΔG° of 0.68 kcal·mol⁻¹ ($K_{D,303-393}/K_{D,303-360} = 0.68$), suggesting again an inhibitory role for the region 303-318, which is offset by the region 361-393 in the peptide 303-393. Removal of 9 C-terminal amino acids from 319-360 reduces the magnitude of ΔG° for tetramerization by 3.10 kcal·mol⁻¹ ($K_{D,319-360}/K_{D,319-351} = 0.17$). Deletion of another 4 amino acids effects a further reduction of the magnitude of

ΔG° of 4.41 kcal·mol⁻¹ ($K_{D,319-351}/K_{D,319-347} = 0.08$). Deletion of 12 N-terminal amino acids from 319-360 also abolishes tetramerization.

CD Spectra of p53 Peptides. The secondary structure of each peptide was estimated by measurement of its CD spectrum. Fig. 3 shows representative spectra of the peptides 319-393, 319-360, and 319AAA-393. The CD spectra of the first two peptides have minima at 208 nm and 222 nm, indicating that these peptides contain a region with α -helical conformation, while the spectrum of 319AAA-393 exhibits no features associated with significant secondary structure. Those peptides which did not exhibit tetramerization—i.e., 335-393, 332-360, and 319AAA-393, also possessed small ellipticity values for θ_{222} . Since the value of θ_{222} reflects percentage of α -helix, these results imply a relationship between the ability to form tetramers and the presence of a significant amount of helical structure (Fig. 2). It is of interest to note that, although peptide 319-351 is 64.1% tetramer at a total concentration of 20 μ M, it has a θ_{222} value of -9988 deg·cm²·dmol⁻¹, while peptide 319-360, which is 89.7% tetramer at this concentration, has a similar θ_{222} value of -9539 deg·cm²·dmol⁻¹. Comparing 319-360 with 319-393, both of which are nearly 90% tetramer at 20 μ M, θ_{222} is -9579 deg·cm²·dmol⁻¹ for 319-360 but is -5959 deg·cm²·dmol⁻¹ for 319-393. These values thus imply that peptide 319-351 has the greatest α -helix content per residue and that the regions to either side have relatively little helical content per residue in comparison.

Coiled-coil dimers or tetramers usually show almost 100% α -helix content (18, 19). However, since the core peptide did not have a high negative ellipticity at 222 nm at 20 μ M, the CD data suggest that the tetramer of p53 does not consist of a typical coiled-coil four-helical bundle, but α -helices appear to be a significant secondary structure.

Determination of Tetramer Orientation. Analogues of the p53 peptide 319-351 were synthesized with acetyl-Cys-Gly-Gly at the N terminus (AC) or benzoyl-Gly-Gly-Cys at the C terminus (BC) for studies on peptide orientation within the tetramer. An equimolar solution of the two analogues was prepared, and the mixed tetramers were cross-linked at the cysteine residues by using 1,6-bismaleimido-hexane and then analyzed by HPLC. If the tetramer had a parallel orientation, it would be expected that two cross-linked homodimers would be the predominant result. The anti-parallel orientation would be expected to produce a mixture of two homodimers and one heterodimer. As shown in Fig. 4, both







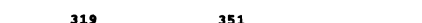


p53 peptides	oligomeric state	$\Delta G^\circ_{293.15}$	K_D	θ_{222}	% tetramer
303-393 	monomer-tetramer	-22.66±0.03	2.34×10 ⁻⁶	-5262	86.4
319-393 	monomer-tetramer	-23.28±0.34	1.64×10 ⁻⁶	-5959	89.5
335-393 	monomer	N/A	N/A	-1528	N/A
303-360 	monomer-tetramer	-21.98±0.08	3.44×10 ⁻⁶	-6370	82.0
319-360 	monomer-tetramer	-23.33±0.14	1.59×10 ⁻⁶	-9539	89.7
319-351 	monomer-tetramer	-20.23±0.02	9.39×10 ⁻⁶	-9988	64.1
319-347 	monomer-tetramer	-15.82±0.04	1.17×10 ⁻⁴	-1428	1.9
332-360 	monomer	N/A	N/A	-1998	N/A
319AAA-393 	monomer	N/A	N/A	-1463	N/A

FIG. 2. Oligomerization status and ellipticity of p53 peptides. ΔG° at $T = 293.15$ K is in kcal·mol⁻¹ (1 kcal = 4.18 kJ). K_D : from the definition of ΔG° , the association constant $K_{14} = \exp(-\Delta G^\circ/RT)$. K_D is commonly defined as the molar concentration of monomer (C_1) when the total concentration (C_T) is such that the molar concentration of monomer equals the molar concentration of oligomer (C_4 for tetramer). With this definition, for monomer-tetramer, $K_D = K_{14}^{-1/3}$. θ_{222} : the ellipticity (deg·cm²·dmol⁻¹) of peptides at a wavelength of 222 nm at 20 μ M and 20°C. % tetramer: the percent tetramer was calculated by solving the equation $C_T = C_1 + 4C_4 = C_1 + 4K_{14}C_1^4$ for C_1 when $C_T = 20$ μ M, expressing all concentrations in terms of molarity of monomer, and then the % tetramer = $100(C_T - C_1)/C_T$. N/A, data not available.

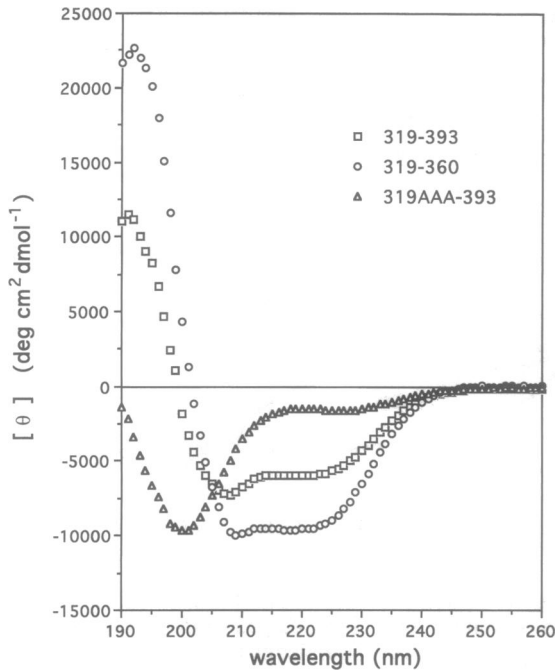


FIG. 3. CD spectra of the p53 peptides. All spectra were recorded with 20 μ M peptide in 50 mM sodium phosphate buffer, pH 7.5 at 20°C.

homodimers and heterodimer were present, at relative concentrations consistent with an anti-parallel orientation. Additionally, equilibrium oxidation experiments were performed in a redox buffer (19). When the disulfide-bridged heterodimer or a mixture of the two homodimers was incubated in the redox buffer, all three possible hetero- and homodimers were observed at equilibrium in both cases (data not shown). These results suggest that the tetramer is a bundle of α -helices in an anti-parallel orientation, as illustrated in Fig. 5. This figure shows the basic domains of C termini of the protein in close apposition with the DNA-binding domains, suggesting a role for the basic domains in the modulation of DNA binding.

DISCUSSION

The work reported here demonstrates that a peptide of 42 amino acids of human p53 (residues 319–360) is the minimum

size required for tetramer formation with a significant α -helix content. The N-terminal truncation of this peptide by 12 amino acids abolishes tetramer formation and decreases the predominantly α -helical structure. Successive C-terminal truncation also reduces tetramer formation.

Other studies have suggested that the C-terminal region is involved in oligomerization (9, 11, 12). Our findings are in general agreement with recent data showing that a domain located in the C-terminal region of p53 (residues 311–363), obtained by partial proteolytic digestion, can oligomerize as a tetramer (9). However, the model proposed by Stürzbecher *et al.* (12) is inconsistent with our data. They found that multiple substitutions of hydrophobic amino acids by either acidic or basic amino acids, within the predicted α -helix of a region corresponding to residues 334–356, abolished any oligomerization of p53. Also, replacement of basic amino acids by alanine or leucine in the region corresponding to residues 363–386 limited p53 oligomerization to dimers, suggesting that p53 dimers will react to form tetramers by bonding of the basic regions. This model is not supported by our findings; a synthetic peptide containing both the predicted α -helix and basic amino acids (residues 335–393) and a variant peptide (319AAA–393) did not form any type of oligomer, whereas the core regions composed of residues 319–347 and 319–351 were able to form tetramers.

The relationship between the structural and thermodynamic properties of the tetramerization domain of p53 is quite interesting. Our CD data indicate that this tetramer is not a typical four-stranded coiled-coil, since the core peptide did not show 100% α -helix even at high concentrations as is seen with a classical leucine zipper (18, 19). Interestingly, the substitutions of three amino acids within the small N-terminal region corresponding to residues 323–330 prevented both the formation of tetramers and the acquisition of an α -helical conformation. Thus, these amino acids are critical for the oligomerization of the p53 core peptide. In addition, residues 331–360, which most likely adopt an α -helical structure, appear to affect the binding free energy for tetramer formation.

Removing residues 361–393 does not have any adverse effect on tetramerization, thus indicating that these residues appear to be functionally neutral in this respect. Truncation of residues 303–318 has relatively little effect. Comparing the peptides 303–393 and 319–393 shows that the tetramerization is enhanced by an increase in ΔG° of 0.6 kcal·mol⁻¹; comparing peptide 303–360 with 319–360 demonstrates an even greater tendency for tetramerization, with ΔG° increased by

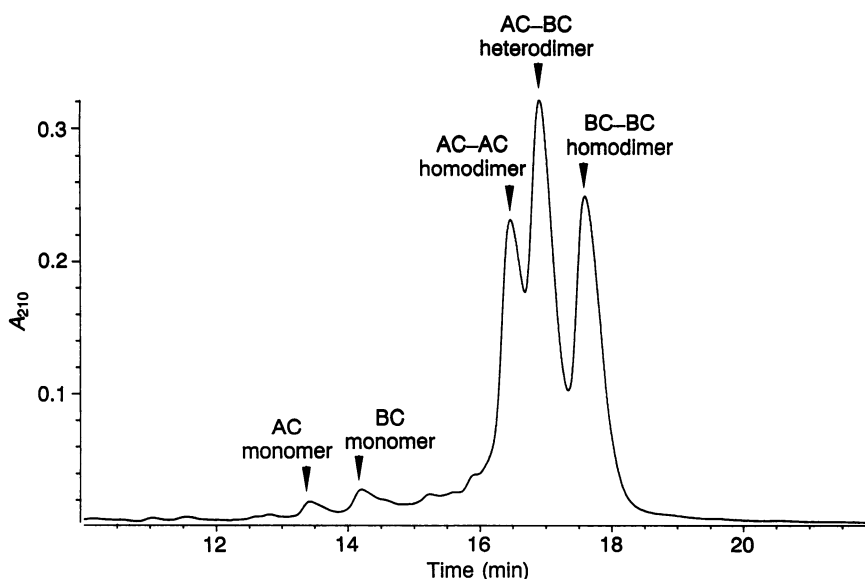


FIG. 4. HPLC analysis of the cross-linked dimers of p53 peptides. The peptides were cross-linked at the cysteine residues by using 1,6-bismaleimido-hexane after the formation of mixed tetramers of AC and BC. Arrows indicate the elution positions of the monomers and the cross-linked dimers.

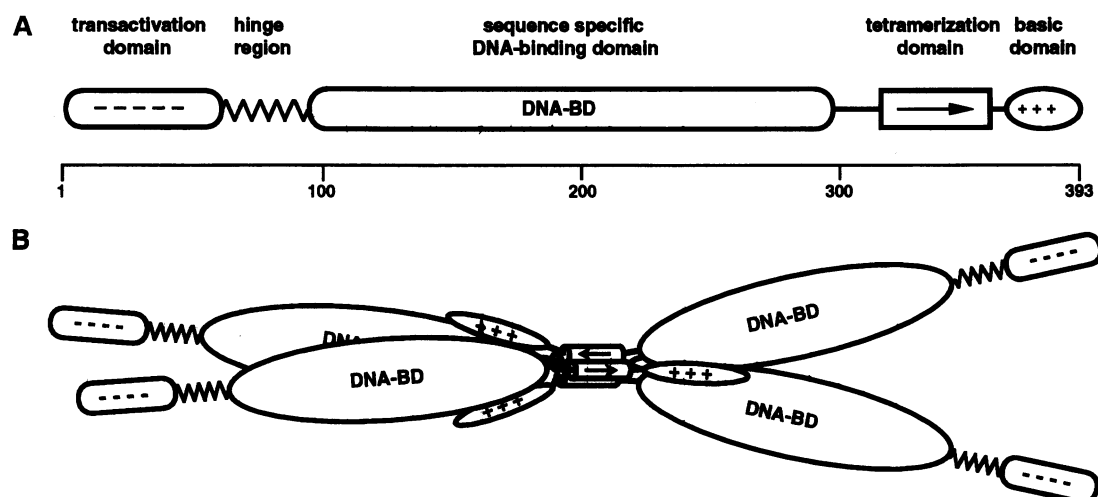


FIG. 5. Model for the anti-parallel orientation of the p53 protein. (A) Primary structure of human p53 protein. (B) Model of the tetrameric arrangement of the p53 protein in the anti-parallel orientation.

1.3 kcal·mol⁻¹. Thus, the region 303–318 reduces affinity but the region 361–393 moderates this reduction. We conclude that 319–360 is the optimal core peptide necessary for tetramer formation and that extension in the N-terminal direction reduces tetramerization while extension in the C-terminal direction has little effect. At the present time, the value of ΔG° for the tetramerization of intact p53 protein is not known at any temperature; a comparison of such values with the values obtained with peptide fragments should be revealing.

These results suggest that the tetramerization of p53 is in part mediated by a coiled-coil type peptide. The analysis of cross-linked tetramers was used to determine whether the monomers had a parallel or an anti-parallel orientation in the tetramers. HPLC analysis of both cross-linked and disulfide-bonded core peptide dimers indicates that the anti-parallel orientation is the preferred conformation. This orientation is not unique to p53 peptides. A recent study of the leucine heptad repeats of *lac* repressor has also shown that the preferred arrangement of the helices in the four-helical bundle structure is anti-parallel (20). In contrast, the x-ray crystal structure of a peptide variant of the GCN4 leucine zipper revealed a parallel four-stranded coiled-coil structure (19).

The tetrameric structure of p53 has important implications for its biological activity. It has been reported that oligomerization of wild-type p53 is required for efficient DNA binding (4, 21). In addition, the C terminus appears to negatively regulate specific DNA binding, since p53 protein lacking the last 30 amino acids of the C terminus exhibits higher affinity for DNA than does wild-type p53 (22). Moreover, phosphorylation of Ser-392 within the C terminus or incubation of the p53 protein with a C-terminus-specific monoclonal antibody (PAb 421) also increases p53 DNA binding. The anti-parallel orientation of the p53 molecules in the tetramer may explain the above phenomena; such an orientation may permit the close apposition of the specific DNA-binding region and the basic 26-amino acid C-terminal region. Since the basic region is responsible for nonspecific DNA binding (23), the negative effect of the C terminus on the specific DNA binding may be due to competition between specific and nonspecific DNA binding. Alternatively, a C-terminal steric effect could block specific DNA binding (Fig. 5B). Consistent with this possibility, the last 26 C-terminal amino acids of human p53 are encoded by a separate exon, suggesting that this may comprise a functionally distinct domain.

Our finding that p53 synthetic peptides form tetramers suggests some interesting future structure/function investigations. We are particularly interested in the idea that such

tetrameric region peptides might disrupt heterodimers composed of mutant and wild-type p53 monomers and that such wild-type p53/peptide complexes might regain DNA-binding ability and biological activity.

This work was supported by the Intramural AIDS Targeted Antiviral Program of the Office of the Director of the National Institutes of Health (to E.A.) and by Research Grants 05453206 and 05780423 from the Ministry of Education, Science and Culture of Japan (to H.K.).

- Levine, A. J., Momand, J. & Finlay, C. A. (1991) *Nature (London)* **351**, 453–456.
- Lane, D. P. & Benchimol, S. L. (1990) *Genes Dev.* **4**, 1–8.
- El-Deiry, W. S., Tokino, T., Velculescu, V. E., Levy, D. B., Parsons, R., Trent, J. B., Lin, D., Mercer, W. E., Kinzler, K. W. & Vogelstein, B. (1993) *Cell* **75**, 817–825.
- Halazonetis, T. D. & Kandil, A. N. (1993) *EMBO J.* **12**, 5057–5064.
- El-Deiry, W. S., Kern, S. E., Pietenpol, J. A., Kinzler, K. W. & Vogelstein, B. (1992) *Nature Genet.* **1**, 45–49.
- Kraiss, S., Spiess, S., Reihnsaus, E. & Montenarh, M. (1991) *Exp. Cell Res.* **192**, 157–164.
- Gannon, J. V., Greaves, R., Iggo, R. & Lane, D. P. (1990) *EMBO J.* **9**, 1595–1602.
- Unger, T., Nau, M. M., Segal, S. & Minna, J. (1992) *EMBO J.* **11**, 1383–1390.
- Pavelech, N. P., Chambers, K. A. & Pabo, C. O. (1993) *Genes Dev.* **7**, 2556–2564.
- Hollstein, M., Sidransky, D., Vogelstein, B. & Harris, C. C. (1991) *Science* **253**, 49–53.
- Milner, J. & Medcalf, E. A. (1991) *Cell* **65**, 765–774.
- Stürzbecher, H. W., Brain, R., Addison, C., Rugbe, K., Remm, M., Grimaldi, M., Keenan, E. & Jenkins, J. R. (1992) *Oncogene* **7**, 1513–1523.
- Albericio, F., Kneib-Cordonier, N., Biancalana, S., Gera, L., Masadsa, R. I., Hudson, D. & Barany, G. (1990) *J. Org. Chem.* **55**, 3730–3743.
- Hojo, H. & Aimoto, S. (1991) *Bull. Chem. Soc. Jpn.* **64**, 111–117.
- Hojo, H. & Aimoto, S. (1992) *Bull. Chem. Soc. Jpn.* **65**, 3055–3063.
- Zamyatnin, A. A. (1984) *Annu. Rev. Biophys. Bioeng.* **13**, 145–165.
- Clarke, E. C. & Glew, D. N. (1966) *Trans. Faraday Soc.* **62**, 539–547.
- O'Shea, E. K., Rutkowski, R. & Kim, P. S. (1989) *Science* **243**, 538–542.
- Harbury, P. B., Zhang, T., Kim, P. S. & Alber, T. (1993) *Science* **262**, 1401–1407.
- Alberti, S., Oehler, S., von Wilcken-Bergmann, B. & Müller-Hill, B. (1993) *EMBO J.* **12**, 3227–3236.
- Shaulian, E., Zauberman, A., Milner, J., Davies, E. A. & Oren, M. (1993) *EMBO J.* **12**, 2789–2797.
- Hupp, T. R., Meek, D. W., Midgley, C. A. & Lane, D. P. (1992) *Cell* **71**, 875–886.
- Wang, T., Reed, M., Wang, P., Stenger, J. E., Mayr, G., Anderson, M. E., Schwedes, J. F. & Tegtmeyer, P. (1993) *Genes Dev.* **7**, 2575–2586.